IEEE Access
Multidisciplinary | Rapid Review | Open Access Journal

Received December 27, 2020, accepted January 7, 2021, date of publication January 14, 2021, date of current version January 25, 2021.

Digital Object Identifier 10.1109/ACCESS.2021.3051843

A HEM-Based Sensitivity Analysis Method for Fast Voltage Stability Assessment in Distribution Power Network

HUIMIN GAO[1], JIANLIN CHEN[1], RUISHENG DIAO[2], (Senior Member, IEEE), AND JING ZHANG[3], (Member, IEEE)

[1]College of Automation, Hangzhou Dianzi University, Hangzhou 310027, China
[2]AI and System Analytics Group, GEIRI North America, San Jose, CA 95134, USA
[3]System Operations, State Grid Zhejiang Electric Power Company, State Grid Corporation of China (SGCC), Hangzhou 310007, China

Corresponding author: Ruisheng Diao (ruisheng.diao@gmail.com)

This work was supported in part by the Natural Science Foundation of Zhejiang Province under Grant LQY19E070001, Grant LY20E070002, and Grant NSF51677047.

ABSTRACT The increased penetration of distributed energy resource and power electronics-based loads cause rapid voltage fluctuations in distribution power networks, affecting secure operation of the grid and threatening high-quality power delivery to customers. It is of great importance to conduct fast and accurate voltage stability assessment for better understanding operational risks and providing effective and timely controls for mitigating the identified risks. Traditionally, Jacobian matrix-based sensitivity analysis methods are used to evaluate voltage stability, however they suffer from ill-conditioned load flow problem caused by numerical stability. To effectively resolve this issue, this paper presents a novel Holomorphic embedding method (HEM)-based approach that can effectively capture sensitivity information for stressed operating conditions when the load flow calculation becomes ill-conditioned. An effective criterion is also proposed to approximate voltage instability point using structural and partial sensitivity information with different orders. The effectiveness of the proposed method is verified via numerical simulations conducted on the IEEE 33-bus and 69-bus test systems.

INDEX TERMS Distribution power grid, holomorphic embedding method, sensitivity analysis, voltage stability assessment.

NOMENCLATURE

$\boldsymbol{Y_{ik}}$	The mutual admittance between buses i and k
$\boldsymbol{V_k}$	The voltage of bus k, in complex form
$\boldsymbol{S_i}$	The power injection into bus i
N	The total number of buses
$Y_{ik,tran}$	The nonground admittance of bus i and bus k
$Y_{i,shunt}$	The ground admittance of bus i
Y_{ii}	The self-admittance of bus i of the nodal admittance matrix
Y_{ik}	the mutual admittance between bus i and bus k of the nodal admittance matrix
$\boldsymbol{c_i}(\boldsymbol{s})$	The s item of holomorphic function of bus i voltage
s	The holomorphic function operator
$\boldsymbol{d_i}(\boldsymbol{s})$	The s item of holomorphic function of bus i inverse voltage
$V_i(\boldsymbol{s})$	The holomorphic function expression of bus i voltage
P_j	The injected active power of bus j
Q_j	The injected reactive power of bus j
$c_i[n]$	The n^{th} item coefficient of holomorphic function of bus i voltage
$\boldsymbol{d_i}[n]$	The n^{th} item coefficient of holomorphic function of bus i inverse voltage
R_L	The load resistance of the two-bus power network
X_L	The load impedance of the two-bus power network
R	The system equivalent resistance of the two-bus power network
X	The system equivalent impedance of the two-bus power network

The associate editor coordinating the review of this manuscript and approving it for publication was Zhouyang Ren.

$\frac{\partial c_i[n]}{\partial P_j}$ The n[th] order voltage sensitivity to active power according to s item of holomorphic function of bus i voltage

$\frac{\partial c_i[n]}{\partial Q_j}$ The n[th] order voltage sensitivity to reactive power according to s item of holomorphic function of bus i voltage

I. INTRODUCTION

Nowadays, more stochastic and dynamic behaviour is observed in today's power network because of the increased penetration of renewable energy, demand response, new market rules, etc. Fluctuations in voltage profiles of distribution power networks may adversely impact the power supply to end users, if not regulated properly; in extreme conditions, local voltage violations may spread towards neighbouring networks, initiate cascading failures and damage power equipment. Thus, fast and accurate assessment of voltage security and stability in real time is of critical importance to enhance situational awareness and enable preventive and corrective controls for mitigating operational risks.

Traditionally, sensitivity-based approaches are often used to assess voltage stability issues and provide voltage control measures, which need to be derived from Jacobian matrices of a distribution network model. Such a method can be affected by the loading conditions, which works well majority of the time when the operating conditions of power grid are less stressed. The obtained sensitivity information is then ranked and processed to design operation logic of voltage controllers and tune their parameters [1]–[3]. Due to the dynamic and stochastic nature of a distribution power network with increased penetration of DERs, the sensitivity-based information needs to be calculated fast enough to capture the changing loading conditions. Thus, the computation speed of deriving accurate sensitivity information in real time becomes critical. Under more stressed or extreme conditions, the Jacobian matrices become ill-conditioned, yielding abrupt increase in the values of voltage control-related sensitivities. This can be used as indicators to assess voltage stability [4]; however, it is still unclear what thresholds to be used to tell true voltage instability due to the numerical stability issues when handling an ill-conditioned matrix. P-V and Q-V curves are typically used to evaluate voltage stability of distribution system, so that the stability margins of different buses are calculated. Those buses with lowest stability margins are then classified as weak buses. The calculations in these methods are complicated and time consuming [5]. Several stability indices are proposed based on the two-bus equivalent model of a distribution network, but most of these indices lack sufficient accuracy under different operation conditions when considering different load models [6]. A new index is presented in [7] to study voltage stability in distribution networks, which can take into account the impact of the presence of DGs and tap changers.

Recently, a novel Holomorphic Embedding Method (HEM) was presented in [8]–[17] to solve AC power flow equations, which can guarantee finding a solution if exists. Unlike Newton's method that requires a relatively good initial guess of the solution, the algorithms in HEM do not depend on initial values and can clearly tell if a solution exists. It revolutionizes the way of performing power flow studies, contingency analysis, voltage stability assessment and so on [11]. The traditional high-order sensitivity uses the AC Newton's approach to calculating second-order voltage sensitivities to reactive power for multiple buses. Such sensitivity focuses on a single index only, which cannot separate linear parts from the non-linear parts [18]. Similarly, the indices based on HELM is proposed [19], which are also using single index values, which is hard to determine voltage stability.

Thus, this paper presents a novel HEM-based approach to computing sensitivities of distribution power networks for voltage and reactive power control, which can effectively overcome the abovementioned issues when dealing with ill-conditioned Jacobian matrices. Two novel concepts including topological-sensitivity and partial-sensitivity with their computational methods are proposed to assess voltage stability and enable fast voltage controls, which is independent of system loading conditions. The key contribution of this paper can be summarized below:

(1) The HEM-based sensitivity method for assessing voltage stability can easily find the noise point of a PV curve comparing to traditional approaches, thus making it more accurate to assess voltage stability under stressed loading conditions.
(2) Using the derived sensitivity information from the proposed approach can quickly tell voltage stability in real time under normal conditions and abnormal conditions. In addition, such an approach does not need to assume proportional load changes when finding the nose points of P-V curves, which is more realistic when handling power network with high penetration of DERs. The time required is much shorter than the traditional methods, since there is no need to calculate the precise nose point of P-V curve.
(3) When assessing voltage stability considering contingencies, there is no need to rerun the entire HEM-based method from scratch. Only a small patch regarding potential topology changes is needed to partially adjust the Jacobian matrices for fast assessment of voltage stability.
(4) The proposed method is general in nature, which can be easily extended to distribution networks with DERs and transmission power network for fast voltage stability assessment.

The remainder of this paper is organized as follow. Section II presents principles of HEM and explains the proposed sensitivity-based methods for voltage stability assessment and control. Section III provides the overall flowchart of the proposed methodology, explains the detailed steps and software implementation. Section IV provides case studies that verify the effectiveness of the approach. Finally, conclusions are drawn in Section V with future work identified.

II. PRINCIPLES OF HEM AND COMPUTATION OF SENSITIVITY FOR VOLTAGE STABILITY ASSESSMENT

A. THE HEM METHOD

For a typical distribution network with only one power source providing electricity. The mathematical equations for power flow computation are given in Eq. (1).

$$\sum_{k=1}^{N} Y_{ik} V_k = \frac{S_i^*}{V_i^*}, \quad i \in m \tag{1}$$

where m is the set of PQ buses. V_k is the voltage of bus k; Y_{ik} is the mutual admittance between buses i and k; S_i is the power injection into bus i; and N is the total number of buses. In such a distribution network, the only PV bus becomes the swing bus and all other buses are modelled as PQ buses. Complex numbers are normally used in power flow calculation to effectively capture the nonlinear relationship between voltage and power injection. Based on the Holomorphic embedding method that also adopts complex numbers for analysis, one can construct a Holomorphic embedding function, shown in Eq. (2).

$$V_i(s) = c_i(s) \sum_{n=0}^{\infty} c_i[n] s^n \tag{2}$$

where s is the operator of embedding coefficient; $c_i(s)$ is the s series expansion of bus i voltage; n is the series order of s; $c_i[n]$ is the n^{th} coefficient of s series order for bus i voltage. Substituting Eq. (2) into Eq. (1) yields:

$$\begin{aligned} \sum_{k=1}^{N} Y_{ik,tran} V_k(s) &= \frac{s S_i^*}{V_i^*(s^*)} - s Y_{i,shunt} V_i(s) \\ Y_{ik,tran} &= \begin{cases} Y_{ii} - Y_{i,shunt} (i = k) \\ Y_{ik} (i \neq k) \end{cases} \end{aligned} \tag{3}$$

where $Y_{i,shunt}$ is the ground admittance of bus i. When s becomes 0, the distribution network is reduced to a single swing bus without power injections on other buses. In this case, a linear power network solution exists. When s becomes 1, it is the solution to the original power flow equations.

Let's assume:

$$\begin{aligned} V_i^{-1}(s) &= d_i(s) = 1/c_i(s) = \sum_{n=0}^{\infty} d_i[n] s^n \\ I_i^{load} &= -Y_{ik,shunt} V_i(s) \end{aligned} \tag{4}$$

Substitute Eqs. (2) and (4) into Eq. (3) yields:

$$\sum_{k=1}^{N} Y_{ik} \sum_{n=0}^{\infty} c_k[n] s^n = s I_i^{load} + s S_i^* \sum_{n=0}^{\infty} d_i^*[n] s^n \tag{5}$$

where I_i^{load} represents the load-to-ground current of bus i. If the distribution network has no grounded loads, then $I_i^{load} = 0 \text{and} Y_{ik,tran} = Y_{ik}$. According to Eq. (5), the 0^{th} order coefficients of the s series are equal; then, one can compute $c_k[0]$ using Eq. (6) and Eq. (7).

$$\sum_k Y_{ik} c_k[0] = 0 \tag{6}$$

$$\begin{aligned} 1 = V(s)V^{-1}(s) &= \left(\sum_{n=0}^{\infty} c[n]s^n\right)\left(\sum_{n=0}^{\infty} d[n]s^n\right) \\ &= c[0]d[0] + s\sum_{m=0}^{1} c[1-m]d[m] \\ &\quad + s^2 \sum_{m=0}^{2} c[2-m]d[m] \\ &\quad + \cdots + s^n \sum_{m=0}^{n} c[n-m]d[m] + \cdots \end{aligned} \tag{7}$$

In Eq. (7), the 0^{th} order coefficients of the s series are equal; then one can obtain:

$$d_k[0] = 1/c_k[0] \tag{8}$$

When the order of s becomes 1, using a similar approach can yield:

$$\sum_{k=1}^{N} Y_{ik} c_k[1] = I_i^{load} + S_i^* d_i^*[0] \tag{9}$$

Then, $c_k[1]$ can be easily computed. Since the 1^{st} order coefficients of s series in Eq. (7) are equal, $d_k[1]$ can be calculated directly from Eq. (10) below:

$$c_k[1] d_k[0] + c_k[0] d_k[1] = 0 \tag{10}$$

Similarly, coefficients of the n^{th} order in the s series can be obtained. Due to the fact that the n^{th} order coefficients are equal in the s series, one can derive Eq. (11) from Eq. (5):

$$\sum_{k=1}^{N} Y_{ik} c_k[n] = S_i^* d_i^*[n-1] \tag{11}$$

Applying the same procedure to Eq. (7) yields:

$$d_i[n] = -\frac{\sum_{m=0}^{n-1} c_i[n-m] d_i[m]}{c_i[0]} \tag{12}$$

Then, $d_i^*[n-1]$ can be computed using Eq. (12); thus, $c_k[n]$ can be calculated by Eq. (11). As the number n grows, all the $c_k[n]$ and $d_k[n]$ can be calculated progressively. In this way, $V_i(s)$ can be computed via Eq. (2). As mentioned above, applying $s = 1$ in Eq. (2) can derive power flow solutions, shown in Eq. (13):

$$V_i(1) = \sum_{n=0}^{\infty} c_i[n] \tag{13}$$

In summary, using HEM to solve power flow equations does not depend upon initial guesses, which can clearly tell whether a solution exists or not. Thus, this approach can be used to assess voltage stability using sensitivity information.

B. CALCULATION OF VOLTAGE SENSITIVITY W.R.T. POWER INJECTION VIA HEM

To effectively assess voltage stability, sensitivity information of voltage with respect to active and reactive power injection is typically used, that is, to compute:

$$\begin{cases} \dfrac{\partial V_i(1)}{\partial P_j} = \sum\limits_{n=0}^{\infty} \dfrac{\partial c_i[n]}{\partial P_j} \\ \dfrac{\partial V_i(1)}{\partial Q_j} = \sum\limits_{n=0}^{\infty} \dfrac{\partial c_i[n]}{\partial Q_j} \end{cases} \tag{14}$$

From the computational process discussed above, the value of $c_i[0]$ has no dependency on power injection, thus,

$$\frac{\partial c_i\,[0]}{\partial P_j} = 0 \quad \text{and} \quad \frac{\partial c_i\,[0]}{\partial Q_j} = 0$$

Taking the partial derivatives of $\sum_k Y_{ik} c_k[1] = I_i^{load} + S_i^* d_i^*\,[0]$ with respective to P_j and Q_j yields:
when j equal to i:

$$\begin{cases} \dfrac{\sum\limits_{k=1}^{N} Y_{ik}\partial c_k\,[1]}{\partial P_j} = d_i^*\,[0] \\ \dfrac{\sum\limits_{k=1}^{N} Y_{ik}\partial c_k\,[1]}{\partial Q_j} = -j * d_i^*\,[0] \end{cases} \tag{15}$$

when j is not equal to i:

$$\begin{cases} \dfrac{\sum\limits_{k=1}^{N} Y_{ik}\partial c_k\,[1]}{\partial P_j} = 0 \\ \dfrac{\sum\limits_{k=1}^{N} Y_{ik}\partial c_k\,[1]}{\partial Q_j} = 0 \end{cases} \tag{16}$$

$\frac{\partial c_i[1]}{\partial P_j}$ and $\frac{\partial c_i[1]}{\partial Q_j}$ can then be obtained by solving Eq. (15) and Eq. (16). The solution process clearly indicates that these two partial derivatives are independent of power flow condition of a distribution power network. They are only dependent upon network topology and electricity distance. Here, they are referred to as **topological-sensitivity**.

From Eq. (12), one can derive Eq. (17) and Eq. (18):

$$d_i\,[1] = -\frac{c_i\,[1]\,d_i\,[0]}{c_i\,[0]} \tag{17}$$

$$\begin{cases} \dfrac{\partial d_i\,[1]}{\partial P_j} = -\dfrac{d_i\,[0]}{c_i\,[0]} * \dfrac{\partial c_i\,[1]}{\partial P_j} \\ \dfrac{\partial d_i\,[1]}{\partial Q_j} = -\dfrac{d_i\,[0]}{c_i\,[0]} * \dfrac{\partial c_i\,[1]}{\partial Q_j} \end{cases} \tag{18}$$

Similarly, taking partial derivatives of Eq. (11) with respect to P_j and Q_j can yield Eq. (19) and Eq. (20):

when j is equal to i:

$$\begin{cases} \dfrac{\sum\limits_{k=1}^{N} Y_{ik}\partial c_k[n]}{\partial P_j} = d_i^*[n-1] + S_i^* * \dfrac{\partial d_i^*[n-1]}{\partial P_j} \\ \dfrac{\sum\limits_{k=1}^{N} Y_{ik}\partial c_k[n]}{\partial Q_j} = -j * d_i^*[n-1] + S_i^* * \dfrac{\partial d_i^*[n-1]}{\partial Q_j} \end{cases} \tag{19}$$

when j is not equal to i:

$$\begin{cases} \dfrac{\sum\limits_{k=1}^{N} Y_{ik}\partial c_k[n]}{\partial P_j} = S_i^* * \dfrac{\partial d_i^*[n-1]}{\partial P_j} \\ \dfrac{\sum\limits_{k=1}^{N} Y_{ik}\partial c_k[n]}{\partial Q_j} = S_i^* * \dfrac{\partial d_i^*[n-1]}{\partial Q_j} \end{cases} \tag{20}$$

From Eq. (12), one can derive:

$$\begin{cases} \dfrac{\partial d_i[n]}{\partial P_j} == -\dfrac{\sum\limits_{m=0}^{n-1} \left(\frac{\partial (c_i[n-m])}{\partial P_j} d_i[m] + c_i[n-m]\frac{\partial d_i[m]}{\partial P_j}\right)}{c_i\,[0]} \\ \dfrac{\partial d_i[n]}{\partial Q_j} == -\dfrac{\sum\limits_{m=0}^{n-1} \left(\frac{\partial (c_i[n-m])}{\partial Q_j} d_i[m] + c_i[n-m]\frac{\partial d_i[m]}{\partial Q_j}\right)}{c_i\,[0]} \end{cases} \tag{21}$$

Note that $\frac{\partial d_i^*[n-1]}{\partial P_j}$ and $\frac{\partial d_i^*[n-1]}{\partial Q_j}$ in Eq. (20) can be obtained using Eq. (21). Then, $\frac{\partial c_i[n]}{\partial P_j}$ and $\frac{\partial c_i[n]}{\partial Q_j}$ can be calculated by Eq. (20). Finally, all the values of $\frac{\partial d_i[n]}{\partial P_j}$ and $\frac{\partial d_i[n]}{\partial Q_j}$ can be easily derived via Eq. (21).

By analyzing the derived equations above, one can find that $\frac{\partial c_i[2]}{\partial P_j}$ and $\frac{\partial c_i[2]}{\partial Q_j}$ are proportional to the first order of load values, because when $n = 2$, the first element of the right hand side of Eq. (19) is constant and the second element is proportional to load values. Such sensitivity information is defined as **first order voltage sensitivity** with respect to load. Similarly, $\frac{\partial c_i[3]}{\partial P_j}$ and $\frac{\partial c_i[3]}{\partial Q_j}$ are proportional to the square of load values; thus, they are named **second order voltage sensitivity** with respect to load. When n becomes large, those sensitivities are defined as **high-order voltage sensitivity** w.r.t. load. Normally, the values of $\frac{\partial c_i[n]}{\partial P_j}$ and $\frac{\partial c_i[n]}{\partial Q_j}$ decrease as n increases and the total nonlinear sensitivity information of voltage w.r.t. power injection, $\frac{\partial V_i}{\partial P_j}$ and $\frac{\partial V_i}{\partial Q_j}$, can be calculated via Eq. (14).

C. ASSESSING VOLTAGE STABILITY USING SENSITIVITY

Steady-state voltage stability assessment is traditionally conducted by Newton-Raphson-based power flow, continuation power flow (CPF) or HEM-based studies that need to calculate PV curves and identify the nose point. The searching process by progressively stressing system loads and observing voltage profiles typically requires a large number of simulations if considering N-1 and/or N-k contingencies. Using Newton's or similar method may suffer from power flow

divergence, which may not be a sufficiently accurate indicator of voltage collapse. In addition, a strong assumption is usually made that system or regional loads change by a uniform pattern when stressing operating conditions, which may not be accurate for real-time implementation in a control center.

As shown in Section II.B, the topological sensitivity is independent of system loads, which is only affected by network topology. Thus, at normal operating conditions with relative strong connection, such sensitivity information can be used to effectively assess voltage stability and provide control suggestions, especially for real-time operation. The voltage sensitivity w.r.t loads can be used to measure the nonlinear relationship between voltage and system load, which can be used to assess voltage stability.

In this work, it is found that at normal operating conditions, higher-order voltage sensitivity values are smaller than topological sensitivity; when network loads are increased, the high-order voltage sensitivity values also increase and will eventually become larger than the 1st order voltage sensitivity value. ***The crossing point between 1st order and higher order sensitivity values becomes a good indicator of voltage collapse point.*** Thus, using the higher-order voltage sensitivity can directly evaluate voltage stability, which takes much less time than traditional methods. This important finding is further illustrated via mathematical derivation for a two-bus power network shown below, the one-line diagram of which is given in Fig. 1.

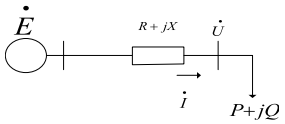

FIGURE 1. One-line diagram of a two-bus power network.

The voltage at the load bus is calculated as $\dot{U} = \dot{E} - \dot{I}(R + jX)$. Let $\dot{E} = E\angle 0^0$, $\dot{U} = U\angle\theta$, then the magnitude of U can be derived as:

$$U = \sqrt{\frac{E^2}{2} - PR - QX \pm \sqrt{(PR+QX-\frac{E^2}{2})^2 - Z^2(P^2+Q^2)}} \tag{22}$$

This forms the basis for PV and QV analysis. When $|Z_L| = |Z|$, $U = \frac{E}{2}$ and the nose point of the PV curve is obtained, indicating:

$$R_L - jX_L = \frac{U^2}{P^2+Q^2}(P - jQ) \tag{23}$$

Namely,

$$\frac{U^4P^2}{(P^2+Q^2)^2} + \frac{U^4Q^2}{(P^2+Q^2)^2} = R^2 + X^2$$
$$E^4/16 = (R^2+X^2)(P^2+Q^2) \tag{24}$$

When $X = 0$, $P = E^4/(4R)$, it indicates the power transfer reaches its maximum, corresponding to the noise point of the PV curve. Using the HEM-based method to calculate voltage sensitivities:

1) From $\sum_{k=1}^{N} Y_{ik}c_k[0] = 0$, one can obtain:

$$\begin{cases} Y_{11}c_1[0] + Y_{12}c_2[0] = 0 \\ Y_{21}c_1[0] + Y_{22}c_2[0] = 0 \end{cases} \tag{25}$$

Since $c_1[0] = E$, $c_2[0] = E$ and $d_2[0] = 1/E$

2) Given $\sum_{k=1}^{N} Y_{ik}c_k[1] = S_i^* d_i^*[0]$,

$$Y_{21}c_1[1] + Y_{22}c_2[1] = S_2^* d_2^*[0] \tag{26}$$

Thus,

$$c_2[1] = (P + jQ) * (R + jX)/E \tag{27}$$
$$d_2[1] = -\frac{c_2[1] * d_2[0]}{c_2[0]} = -\frac{(P - jQ)(R + jX)}{E^3} \tag{28}$$

3) From $\sum_k Y_{ik}c_k[2] = S_i^* d_i^*[1]$, one can obtain

$$c_2[2] = -\left(P^2 + Q^2\right) * \left(R^2 + X^2\right)/E^3 \tag{29}$$
$$d_2[2] = -\frac{c_2[2] * d_2[0] + c_2[1] * d_2[1]}{c_2[0]} = \frac{(P^2+Q^2) * (R^2+X^2) + (P - jQ)^2(R + jX)^2}{E^5} \tag{30}$$

4) From $\begin{cases} Y_{11}c_1[3] + Y_{12}c_2[3] = S_1^* d_1^*[2] \\ Y_{21}c_1[3] + Y_{22}c_2[3] = S_2^* d_2^*[2] \end{cases}$, one can obtain

$$c_2[3] = \frac{S_2^* d_2^*[2]}{Y_{22}} = \frac{2[(PR+QX) + j(XP - QR)]\left[(PR+QX)^2 - j\left[XR\left(P^2 - Q^2\right) + QP\left(X^2 - R^2\right)\right]\right]}{E^5}$$

Thus, with $c_2[0]$ through $c_2[3]$, one can obtain:

$$\frac{dc_2[0]}{dQ} = 0$$
$$\frac{dc_2[1]}{dQ} = \frac{X - jR}{E}$$
$$\frac{dc_2[2]}{dQ} = \frac{-2Q}{E^2}(R^2 + X^2)$$
$$\frac{dc_2[3]}{dQ} = 2[[X - jR][(PR + QX)^2 - j[XR(P^2 - Q^2) + QP(X^2 - R^2)]] + [(PR+QX)+j(XP-QR)][2(PR+QX)X - j[-2QXR + P(X^2 - R^2)]]/E^5$$

Let $R = 0$, $\frac{dc_2[2]}{dQ} = \frac{dc_2[3]}{dQ}$, yields:

$$\frac{(3Q^2X^3 + P^2X^3)}{E^5} = \frac{-QX^2}{E^3} \Rightarrow 3XQ^2 + E^2Q + P^2X = 0$$

Thus, since the equation has real number solution, we can obtain:

$$P^2 \leq \frac{(c_2\,[0])^4}{12X^2} = \frac{E^4}{12X^2}$$

This criterion is close to the PV nose point indicated by $E^4/16 = (R^2 + X^2)(P^2 + Q^2)$. In fact, higher order sensitivity crossing points are closer to noise points, which are verified via numerical simulations in Section IV.

III. PROPOSED HEM-BASED SENSITIVITY CALCULATION METHOD TO ASSESS VOLTAGE STABILITY

The overall flowchart of the proposed HEM-based sensitivity calculation method for assessing voltage stability is given in Fig. 2, which consists of several key steps.

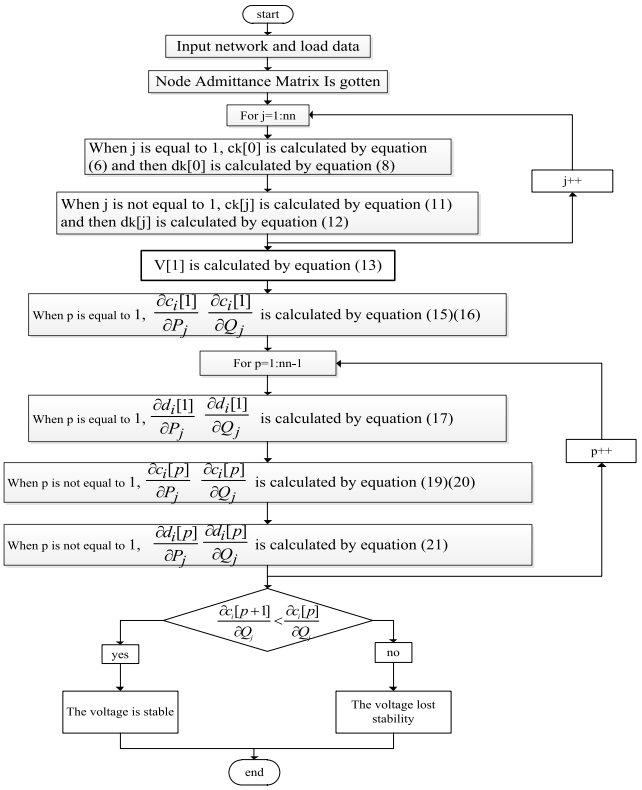

FIGURE 2. Main flowchart of the proposed method.

Step 1: pre-processing of power network model and obtain node admittance matrix.

Step 2: computation of c_k and d_k values using Equations (6) through (12).

Step 3: calculation of partial derivatives to form sensitivity information using Equations (13) through (21).

Step 4: applying sensitivity info for voltage stability assessment. If higher-order sensitivity is bigger than lower-order sensitivity, then it indicates voltage instability. For providing voltage control in real-world implementation, one can use certain margins as the difference between higher-order sensitivity and lower-order sensitivity, before activating control actions.

IV. CASE STUDIES

To verify the effectiveness of the proposed method, two standard distribution test systems are used, including the IEEE 33-bus model and IEEE 69-bus model. The test performance with discussion is given in the subsequent sections. The proposed method is developed using MATALB scripts that can run on Windows Desktop or Laptop with Intel Core I7-8565U CPU at 1.8 GHz and 8GB RAM.

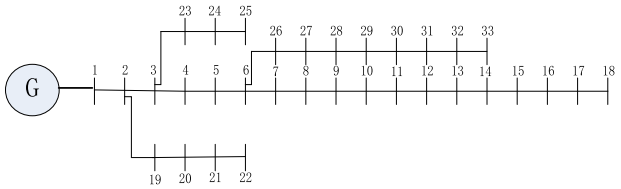

FIGURE 3. One-line diagram of the IEEE 33-bus distribution network.

A. CASE 1: IEEE 33-BUS MODEL

The one-line diagram of the IEEE 33-bus model is provided in Fig. 3 with details given in [12]. The power flow solution using Holomorphic embedding method is compared with the forward/backward sweep-based method, with solution errors depicted in Fig. 4. As can be seen, the solution values of the two methods are sufficiently close, which verifies the accuracy of HEM in providing power flow solutions.

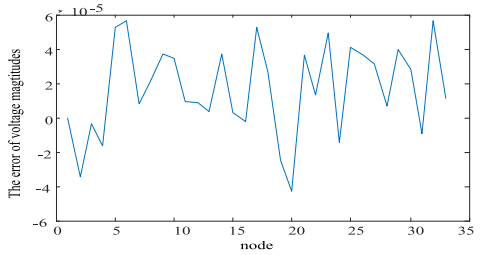

FIGURE 4. Comparison of voltage magnitude in power flow solution between HEM and Forward/Backward sweep method.

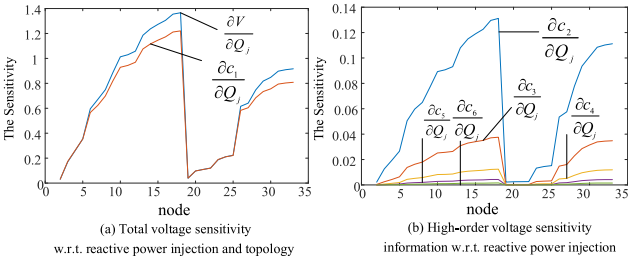

FIGURE 5. Voltage sensitivity w.r.t. reactive power for the base case using HEM.

The voltage sensitivity information based on HEM is calculated for the base case and shown in Fig. 5, the values of which are verified against the ones calculated via perturbation method as shown in Fig.6. It can be observed from Fig. 5(a) that the difference between $\frac{\partial V}{\partial Q_j}$ and $\frac{\partial C1}{\partial Q_j}$ is relatively small and $\frac{\partial C1}{\partial Q_j}$ is independent of system loads, indicating the total voltage sensitivity w.r.t. reactive power injection can be approximated by $\frac{\partial C1}{\partial Q_j}$ that takes much less time to compute.

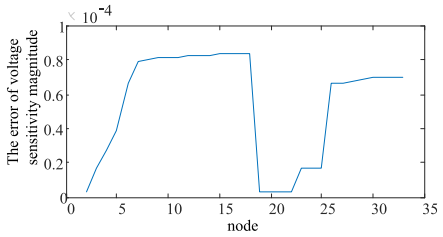

FIGURE 6. Comparison of voltage sensitivity magnitude between the proposed method and the perturbation method.

It also indicates that at normal operating conditions, voltage sensitivity is more affected by system topology and electrical distance, less affected by system loads. From Fig. 5(b), one can observe that at normal operating conditions $\frac{\partial C1}{\partial Q_j}$ is proposal to system loads and the values of $\frac{\partial C2}{\partial Q_j}$, $\frac{\partial C3}{\partial Q_j}$, …, $\frac{\partial C6}{\partial Q_j}$ gradually decreasing, representing the nonlinear portion of voltage sensitivity w.r.t. system load. It is also interesting to point out that the patterns are similar among $\frac{\partial C2}{\partial Q_j}$ through $\frac{\partial C6}{\partial Q_j}$.

From Fig. 6, it can be seen that the errors of the results obtained by these two methods are extremely small, which verify the accuracy of the proposed method.

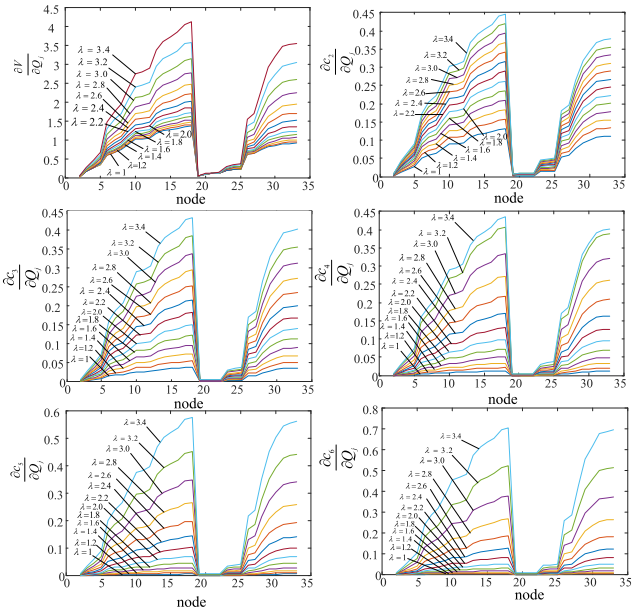

FIGURE 7. Voltage sensitivity information for various levels of system loads (λ).

From Fig. 7, when system loads are increased, the ranking among different orders of voltage sensitivity remains the same, indicating a strong network connection at the base case. In this case, the ranking of voltage sensitivity heavily depends on network topology. $\frac{\partial C1}{\partial Q_j}$ remains unchanged during the stressing process of system load, but the values of $\frac{\partial C2}{\partial Q_j}$ through $\frac{\partial C6}{\partial Q_j}$ increase dramatically with system loads. More importantly, the ranking among $\frac{\partial C2}{\partial Q_j}$ through $\frac{\partial C6}{\partial Q_j}$ can change as well, which provides a good indicator of voltage instability.

Another study is conducted to evaluate the change in voltage sensitivity when increasing the reactive power consumption at bus 18 only. The obtained sensitivity information is plotted in Fig. 8. It clearly shows that the ranking of voltage sensitivity does not change when stressing system loads.

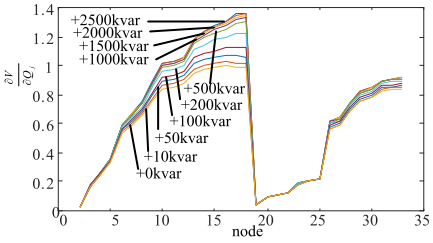

FIGURE 8. Voltage sensitivity w.r.t. load change at bus 18.

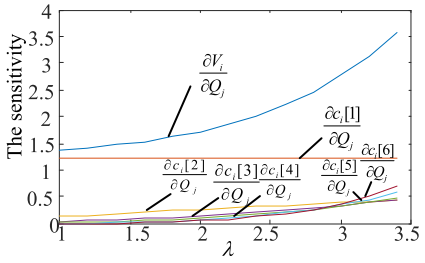

FIGURE 9. Change of voltage various sensitivity w.r.t. system loading levels.

Fig. 9 provides the trend of voltage sensitivity values when system loads are increased. As system is more stressed, the values of $\frac{\partial C2}{\partial Q_j}$ through $\frac{\partial C6}{\partial Q_j}$ also increase, until reaching a loading condition where crossing of multiple partial voltage sensitivity curves occur. It is found that this crossing point is consistent with the nose point calculated using the traditional PV curve. After this crossing point, different partial sensitivity values increase significantly with their ranking swapped, providing an effective indicator of voltage instability. Based on these findings, one important criterion can be formed:

$$\textit{When } \frac{\partial C2}{\partial Q_j} \geq \frac{\partial C3}{\partial Q_j}, \textit{ it indicates voltage instability}$$

This criterion is relatively easy and fast to compute, which is suitable for real-time application.

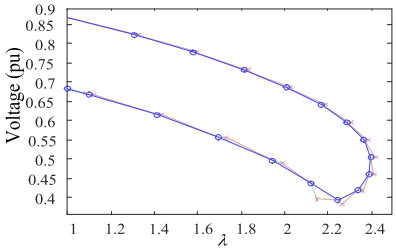

FIGURE 10. Voltage profiles with increased system loads.

To verify the effectiveness of using this criterion for voltage stability assessment, a series of numerical studies by MATPOWER are conducted, with results shown in Fig.10. From Fig.10, we can see the maximum system load when reaching voltage instability is approximately 2.4 times of the base load.

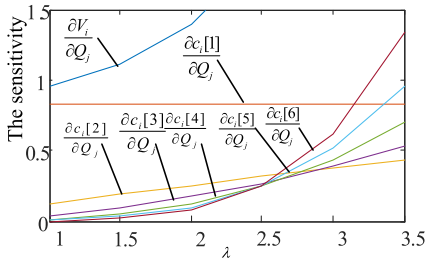

FIGURE 11. Voltage sensitivities at various buses when increasing system loads.

Fig. 11 provides voltage sensitivity variables w.r.t. reactive power at bus 30. As can be seen from the crossing points of these sensitivity curves, they all point to the loading level is around 2.5 times of the base load, which verifies the above criterion for fast voltage stability assessment.

The computation time required by the proposed HEM-based sensitivity method and the required time by MATPOWER is compared in Table 1. From Table 1, we can find the required time by proposed method is much smaller than the time used by MATPOWER because the method to judge voltage stability doesn't need to solve many power flow equations.

In real-time voltage stability assessment, one can use the error values between higher-sensitivity and lower-sensitivity. If the error is more than zero, it means the voltage is stable. If the error is less than zero with a certain margin, it indicates voltage instability. The maximum load margin does not need to be calculated, which is not easily to be obtained because of the DERS and FACT devices. So the method assess the voltage stability is simple and quick, which can be used for real-time voltage stability assessment in distribution systems.

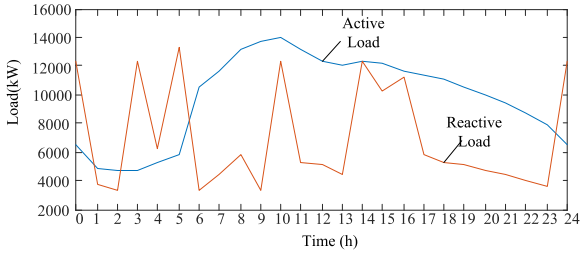

FIGURE 12. Daily load curve of the IEEE 33-bus system.

Figure 12 shows the daily load curve for the 33-bus system to demonstrate the effectiveness of the proposed approach for various system operating conditions. Then, the error values between higher-sensitivity and lower-sensitivity are calculated for selected time stamps during the typical day for assessing voltage stability.

From Figure 13, one can observe that the error values between 6th order sensitivity and 5th order sensitivity is greater than zero, which means that the system loses voltage stability at 10, 14 and 16 O'clock when the system is stressed with higher active power and reactive power injection. It can also be found that the system loses voltage stability at 3 and 5 O'clock because the reactive power injection is high while

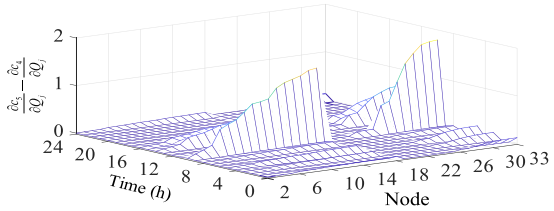

(a) the errors between 6th order sensitivity and 5th order sensitivity

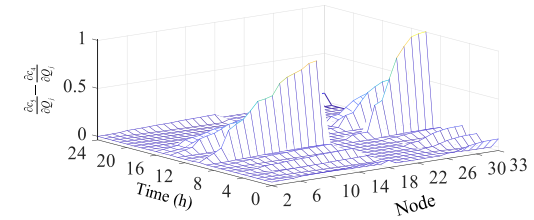

(b) the errors between 5th order sensitivity and 4th order sensitivity

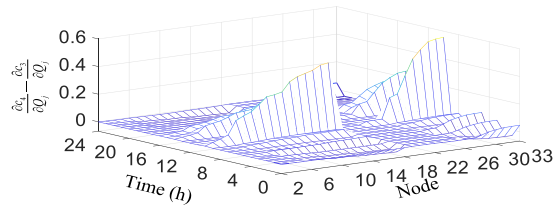

(c) the errors between 4th order sensitivity and 3rd order sensitivity

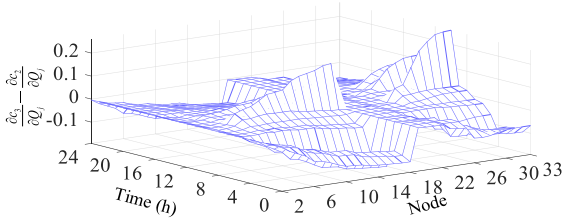

(d) the errors between 3rd order sensitivity and 2nd order sensitivity

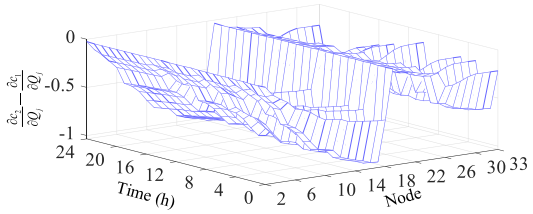

(e) the errors between 2nd order sensitivity and 1st order sensitivity

FIGURE 13. The error values between higher order sensitivity and lower order sensitivity.

TABLE 1. Computation time required to identify voltage instability for the IEEE 33-bus test system.

Continuation Power Flow in MATPOWER	HEM-Based Method
0.578980 s	0.038309 s

active power consumption is light. If using CPF method, such voltage instability points cannot be determined. A threshold regarding the error values between higher-order and lower-order sensitivities can be used to prevent voltage instability for a distribution system with DERs, which is easy to compute and implement.

B. CASE 2: IEEE 69-BUS MODEL

The voltage sensitivity information based on HEM for the IEEE 69-bus model is calculated for the base case and shown in Fig. 14, the values of which are verified against the ones calculated via perturbation method.

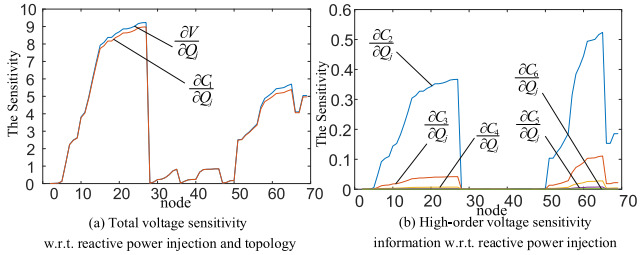

FIGURE 14. Voltage sensitivity w.r.t. reactive power for the base case using HEM.

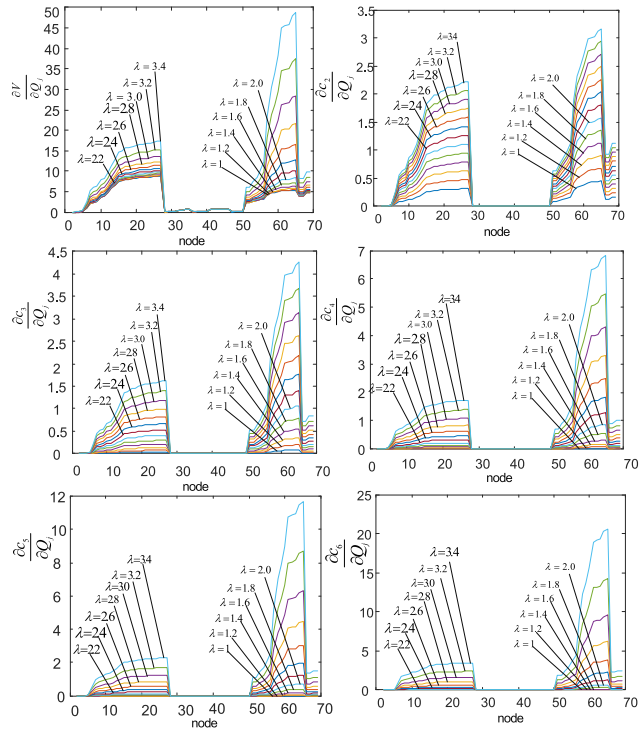

FIGURE 15. Voltage sensitivity information for various levels of system loads (λ).

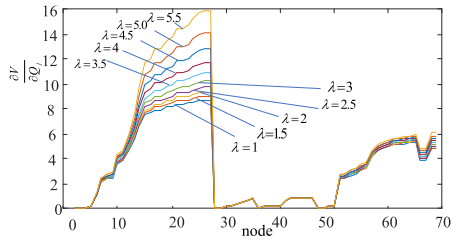

FIGURE 16. Voltage sensitivity w.r.t. load change at bus 22,23,24,25,26.

We increase the system load by λ coefficient proportionality and then the obtained voltage sensitivities are shown in Fig.15. Similar observations and trends are obtained, compared to the IEEE 33-bus system model. Similarly, the voltage sensitivity at buses 22,23,24,25 and 26 with respect to reactive power consumption is plotted in Fig. 16. It further verifies that the ranking of voltage sensitivity does not change when stressing system loads.

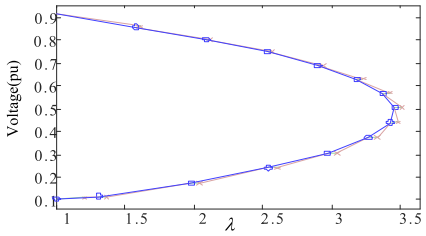

FIGURE 17. P-V curve obtained using the continuation power flow method in MATPOWER, for bus 61.

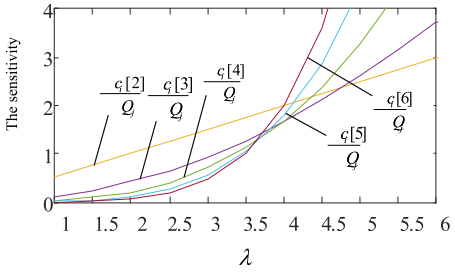

FIGURE 18. Voltage sensitivities at bus 61 when increasing system loads.

To verify the effectiveness of the proposed method in determining voltage stability, the P-V curve for bus 61 is calculated using the continuation power flow methods provided by MATPOWER, shown in Fig. 17, where **y** axis represents bus voltage magnitude and **x** axis stands for the load change coefficient, λ. At the nose point, the voltage magnitude reaches 0.5 pu and λ is approximately 3.4. Using the proposed method to calculate voltage sensitivities at bus 61 while increasing system loads can obtain the curves shown in Fig.18. From Fig. 18, we can observe that the sensitivity values of $\frac{\partial C2}{\partial Q_j}$, $\frac{\partial C3}{\partial Q_j}$, ... $\frac{\partial C6}{\partial Q_j}$ all increase with the value of λ. When λ is reaches 3.5, $\partial C_6/\partial Q_j$ is greater than $\partial C_3/\partial Q_j$. This value is approximately equal to the value obtained by MATPOWER. This means that we can use the crossing point of $\frac{\partial C3}{\partial Q_j}$ and $\frac{\partial C6}{\partial Q_j}$ as an effective indicator of voltage instability.

The computation time used by the proposed HEM-based method and MATPOWER to determine voltage instability is compared in Table 2. As can be seen, the time used by the proposed HEM-based method is much shorter than the time used by MATPOWER, as expected. It is worth mentioning that in the proposed method, sensitivity values are mostly derived from power grid topology information, which may change for different operating conditions. The controlling parameters of the proposed method include reactive power and active power injection from system loads or renewable energy. With such information available from SCADA or EMS in real time, the corresponding sensitivity values can be directly obtained by the proposed method.

TABLE 2. Computation time required to identify voltage instability for the IEEE 69-bus test system.

Continuation Power Flow in MATPOWER	HEM-Based Method
0.640968 s	0.108884 s

V. CONCLUSION AND FUTURE WORK

To overcome the known issues when assessing voltage stability for distribution networks, this paper presents a novel HEM-based approach to computing various sensitivity information, including topological-sensitivity and partial-sensitivity for fast voltage stability assessment. Detailed mathematical equations regarding voltage sensitivity calculation are provided. The proposed method provides a promising way of using topological information only for voltage stability assessment without progressively stressing system loads for voltage stability assessment. The effectiveness of this approach is verified via numerical studies conducted on the IEEE 33-bus and IEEE 69-bus distribution power network models.

In future work, we plan to further improve our methodology and test it on larger power network models with realistic operating features and DERs for voltage control and optimization.

REFERENCES

[1] S. Li, Y. Tan, C. Li, Y. Cao, and L. Jiang, "A fast sensitivity-based preventive control selection method for online voltage stability assessment," *IEEE Trans. Power Syst.*, vol. 33, no. 4, pp. 4189–4196, Jul. 2018.

[2] K. Alzaareer, M. Saad, H. Mehrjerdi, C. Z. El-Bayeh, D. Asber, and S. Lefebvre, "A new sensitivity approach for preventive control selection in real-time voltage stability assessment," *Int. J. Electr. Power Energy Syst.*, vol. 122, Nov. 2020, Art. no. 106212.

[3] N. Amjady and M. Esmaili, "Application of a new sensitivity analysis framework for voltage contingency ranking," *IEEE Trans. Power Syst.*, vol. 20, no. 2, pp. 83–973, May 2015.

[4] D. Hazarika, "New method for monitoring voltage stability condition of a bus of an interconnected power system using measurements of the bus variables," *IET Gener., Transmiss. Distrib.*, vol. 6, no. 10, pp. 977–985, 2012.

[5] C.-Y. Lee, S.-H. Tsai, and Y.-K. Wu, "A new approach to the assessment of steady-state voltage stability margins using the P–Q–V curve," *Int. J. Electr. Power Energy Syst.*, vol. 32, no. 10, pp. 1091–1098, Dec. 2010.

[6] S. Banerjee, D. Das, and C. K. Chanda, "Voltage stability of radial distribution networks for different types of loads," *Int J Power Energy Convers*, vol. 5, no. 1, pp. 70–87, 2014.

[7] S. E. Sadeghi and A. A. Foroud, "A new approach for static voltage stability assessment in distribution networks," *Int. Trans. Electr. Energy Syst.*, vol. 30, no. 3, Mar. 2020, Art. no. e12203.

[8] S. Rao, Y. Feng, D. J. Tylavsky, and M. K. Subramanian, "The holomorphic embedding method applied to the power-flow problem," *IEEE Trans. Power Syst.*, vol. 31, no. 5, pp. 3816–3828, Sep. 2016.

[9] A. Trias and J. L. Marín, "The holomorphic embedding loadflow method for DC power systems and nonlinear DC circuits," *IEEE Trans. Circuits Syst.*, vol. 63, no. 2, pp. 322–333, Feb. 2016.

[10] B. Wang, C. Liu, and K. Sun, "Multi-stage holomorphic embedding method for calculating the power-voltage curve," *IEEE Trans. Power Syst.*, vol. 33, no. 1, pp. 1127–1129, Jan. 2018.

[11] R. Yao, K. Sun, D. Shi, and X. Zhang, "Voltage stability analysis of power systems with induction motors based on holomorphic embedding," *IEEE Trans. Power Syst.*, vol. 33, no. 1, pp. 1127–1129, Mar. 2018.

[12] M. E. Baran and F. F. Wu, "Network reconfiguration in distribution systems for loss reduction and load balancing," *IEEE Trans. Power Del.*, vol. 4, no. 2, pp. 1401–1407, Apr. 1989.

[13] C. Liu, B. Wang, X. Xu, K. Sun, D. Shi, and C. Bak, "A multi-dimensional holomorphic embedding method to solve AC power flows," *IEEE Access*, vol. 5, pp. 25270–25285, 2017.

[14] H.-D. Chiang, T. Wang, and H. Sheng, "A novel fast and flexible holomorphic embedding power flow method," *IEEE Trans. Power Syst.*, vol. 33, no. 3, pp. 2551–2562, May 2018.

[15] M. Basiri-Kejani and E. Gholipour, "Holomorphic embedding load-flow modeling of thyristor-based FACTS controllers," *IEEE Trans. Power Syst.*, vol. 32, no. 6, pp. 4871–4879, Nov. 2017.

[16] Y. Zhu, D. Tylavsky, and S. Rao, "Nonlinear structure-preserving network reduction using holomorphic embedding," *IEEE Trans. Power Syst.*, vol. 33, no. 2, pp. 1926–1935, Mar. 2018.

[17] C. Liu, K. Sun, B. Wang, and W. Ju, "Probabilistic power flow analysis using multidimensional holomorphic embedding and generalized cumulants," *IEEE Trans. Power Syst.*, vol. 33, no. 6, pp. 7132–7142, Nov. 2018.

[18] A. Berizzi, C. Bovo, M. Merlo, G. Callegari, M. Porcellini, and M. Pozzi, "Second order sensitivities for constrained reactive optimal power flow," in *Proc. 43rd Int. Universities Power Eng. Conf.*, Padua, Italy, 2008, pp. 1–7.

[19] S. Rao, D. Tylavsky, V. Vittal, W. Yi, D. Shi, and Z. Wang, "Fast weak-bus and bifurcation point determination using holomorphic embedding method," in *Proc. IEEE Power Energy Soc. Gen. Meeting (PESGM)*, Aug. 2018, pp. 1–5.

HUIMIN GAO was born in Jiangxi, China, in 1978. She received the B.S. and M.S. degrees from Zhengzhou University, China, in 2000 and 2003, respectively, and the Ph.D. degree from Zhejiang University, China, in 2006, all in electrical engineering. She is currently an Associate Professor with the Department of Electrical Engineering, Hangzhou Dianzi University. Her main research interest includes power system stability, control, and planning.

JIANLIN CHEN was born in Jiangxi, China, in 1994. She received the B.S. degree in electrical engineering from East China Jiaotong University, China, in 2016. She is currently pursuing the master's degree in control engineering with Hangzhou Dianzi University. Her main research interest includes power system stability, control, and planning.

RUISHENG DIAO (Senior Member, IEEE) received the Ph.D. degree in electrical engineering from Arizona State University, in 2009. He is currently the Deputy Department Head of AI and System Analytics, GEIRI North America. His research interests include high-fidelity simulation techniques and AI-based methods for grid operations. He serves as an Associate Editor for IEEE TRANSACTIONS ON POWER SYSTEMS, IEEE ACCESS, IEEE POWER ENGINEERING LETTERS, and *IET Generation, Transmission and Distribution*. He was the recipient of the 2018 Research and Development 100 Awards.

JING ZHANG (Member, IEEE) was born in Henan, China, in 1980. He received the Ph.D. degree in electrical engineering from Zhejiang University, Hangzhou, China, in 2009. He is currently a Senior Engineer with the State Grid Zhejiang Electric Power Company. His main research interests include power system stability, HVDC and FACTS, and signal processing.